MECHANISM OF LOW CYCLE SMALL SURFACE CRACK PROPAGATION

N.A. Makhutov*, I.V. Makarenko*

The methodology to study kinetics of surface, semi-elliptic, inclined small-cycle cracks is developed. The calculation model for surfaces of cracks initiated from semi-elliptic multi-directional crack-type flaws is proposed and discussed. Formulas, obtained on the basis of fracture strain criteria, with the purpose to determine stress-strain conditions along the front of cracks can be used when selecting analysis approaches and design factors based on fracture-resistance parameters.

INTRODUCTION

In many cases, fracturing of structures subjected to cyclic, rated, elasto-plastic loadings occurs as a result of presence, initiation and propagation in their elements of surface, semi-elliptic, multi-directional small-cycle cracks. Therefore, to predict structure service life it is necessary to know the laws of crack propagation. Until now, the literature on crack analysis dealt mainly with cracks under mixed loadings on the basis of the elasticity theory (for instance, Sih (1) and a number of other works). The general character of stress-strain conditions along the front of elliptic and surface semi-elliptic cracks under random rated loadings as well as strain mathematic expressions for individual cases of tangential loadings uniformly spread over elliptic cracks, were also discussed. Many papers elucidate the problem of the growth of fatigue surface semi-elliptic cracks as a result of sur-

* USSR Academy of Science, Mechanical Engineering Research Institute, Moscow.

face-perpendicular loadings (Scott and Thorp (2), Hodulak et. al. (3) and some others). In such case, development of the crack form is often used as a diagnostic method to determine accuracy of solutions for stain intensity factors related to rated elastic loadings. At present, there are practically no publications dealing with kinetics of surface, semi-elliptic, inclined, small-cycle cracks. The present paper based on the proposed methodology, discusses the results of studying kinetics of the above cracks having various initial orientations. Taking fracture strain criteria (Makhutov (4)) and the proposed calculation diagram for developed surface cracks as a basis, we obtained compact (i.e. suitable for engineering designs) elasto-plastic solutions for strain and stress intensity factors related to the front of investigated cracks.

Methodology to study kinetics of surface semi-elliptic inclined small-cycle cracks

Experiments with kinetics and geometry of small-cycle surface cracks developing from initial multidirectional semi-elliptic thin notches made through polished surface on pipe samples from austenite cycle-stable stainless steels of 08Х18Н10Т type, and perlite cyclically unstable refractory steels of 12Х2МФА type, were done by subjecting the samples to soft axial saw-like loadings (central compression-tension) with cycle asymmetry factor R = -1, and loading frequency 0.01 Hz. Up to 12 semi-elliptic multi-directional thin notches 0.1 - 1 mm deep were made on the surface of each sample by means of electroerosion (Fig. 1); spacing between them corresponded to the condition of non-interaction until the stage of significant damage of the sample (Makhutov and Makarenko (5)). The depth of initial notches (smaller semi-axes of ellipses) varied in the range $b = (0.06\text{-}0.30)t$, and their lengths on sample surfaces (greater axes) - in the range $2a = (0.003\text{-}0.045)l_p$, where t and l_p - are wall thicknesses and external surface perimeters of the samples respectively. Angles between the planes of initial semi-elliptic notches and sample cross-sections varied from $\beta = 0$ to $\beta = \pi/2$, and the width of notches was 0.05-0.10 mm. To make notches, brass foil electrodes were used, whose width was chosen to be equal to the given length of notches on the sample surface (2a). Geometry of the electrode ends (outline) was semi-elliptic with semi-axes a_1 and b_1. a_1 and b_1 constants were given according to required values of the initial notch semi-axes (a,b). $b:b_1$ ratio depends on both mechanical properties and size of foil electrodes, and performance of an electro-

erosion unit. Using square-type reticule (on polished sample surfaces) plotted at the tops of notches with steps of 0.05 - 0.10 mm (Makhutov (4)), and a special optical system it was possible to measure local elasto-plastic strains in the crack propagation zones. Crack growth length, coordinates of their tops and crack openings on the sample surface were measured with accuracy of 0.001 mm, and distances between the reticule lines - with accuracy of $0.5 \cdot 10^{-4}$ mm. Crack growth in depth and their surface configuration were determined by means of colorants, introduced into cracks during the tension semi-cycle after certain numbers of loadings cycles.

The characteristic configuration of crack surfaces at the initial stage of its development is shown in the form of isometric chart on Fig. 2. On the sample surface, cracks develop parallel to the normal cross-section rate, and by the depth their surfaces acquire a peculiar distortion. With the initial notch angle β approaching $\pi/2$, the surface of developing crack is changing (while retaining all features shown on Fig. 2), and when $\beta = \pi/2$, it assumes the semi-elliptic form. That means that at the stage under consideration, the crack growth path is determined mainly by the local loading component according to model 1. However, the initial notch angle has a significant effect on initiation of cracks and the rate of their propagation. Fig. 3 shows a characteristic kinetic change of calculated semi-axes crack surfaces under consideration; $\bar{\sigma}_m = \pm 1.04$ (where $\bar{\sigma}_m = \sigma_m / \sigma_{0.2}$). It is clearly shown that a lesser angle β results in decrease of the crack growth rate, as well as that the rate in direction of axis b is greater than the rate in a* direction. This is illustrated in Fig. 4.

Calculated and experimental analysis of stress-strain conditions on crack fronts. On the basis of fracture strain criteria (Makhutov (4)), Fig. 5 shows a graphic comparison of calculated and experimental values of the range of relative elasto-plastic strains in surface points of crack fronts (elliptic angle $\phi = 0$) with various β; on pipe samples having diameters d/D = 0.6 and D = 50 mm from 08X18H10T steel. The calculation model for developed crack surfaces, shown on Fig. 2, was used. The calculation model represents a semi-elliptic inclined surface with a given angle β^* and given semi-axes $b^* = b = ok$, $a^* = ob_1 = ob_2$. The range of relative elasto-plastic strain on the crack front was calculated by the following formula (Makhutov (4))

$$\Delta \bar{e}^{*}_{jz} = 2 \frac{(\Delta \bar{K}^{*}_{I(\varphi)})^{p^{(k)}_{ke}}}{(2\pi r^{*})^{p^{(k)}_{re}}} \cdot \bar{e}^{*}_{m} \cdot f(r^{*}/l^{*}_{jx}) \quad \ldots\ldots \quad (1)$$

where $\bar{K}^{*}_{I(\varphi)} = K^{*}_{I(\varphi)}/\sigma_{0.2}$ - the relative stress intensity factor in the area of rated elastic strains e_m, ($\bar{e}_m = e_m/e_{0.2}$), and it is calculated by formulas (Scott and Thorp (2), Makhutov (4)) which correlate well at b^{*}, a^{*}, β^{*} parameters; $f(r^{*}/l^{*}_{jx})$ - correction function depending on r^{*} coordinate of the poit under study in the minimum section; $P^{(k)}_{ke}$, $P^{(k)}_{re}$ - parameters of fracture strain criteria (4); $\bar{e}^{*}_{m} = \bar{e}_{m} \cdot \mathrm{Sin}^{2} \beta^{*}$; experimental value of elasto-plastic relative strain range near the front $(\Delta \bar{e}^{*}_{jz})^{exp} = (\Delta \bar{e}_{jz})^{exp} \cdot \mathrm{Sin}^{2} \beta^{*}$, j - angle β parameter, X, Y, Z - direction of coordinate axes (Fig.1). It follows that provided a relatively adequate calculation model for developed crack surfaces in their surface point of the front $\varphi = 0$ (Fig. 5), and knowing $\bar{K}^{*}_{I(\varphi)}$ on crack fronts in the elastic area of rated loadings (2,4), it is possible, using fracture strain criteria (4) to write an elasto-plastic solution for intensity factors of strain on crack fronts $(\bar{K}^{*}_{Ie})_{\varphi}$. The range of the relative value $(\bar{K}^{*}_{Ie})_{\varphi}$ according to (4) is

$$(\Delta \bar{K}^{*}_{Ie})_{\varphi} = 2 \frac{(K^{*}_{Ie})_{\varphi}}{\sigma_{0.2}} = 2 \bar{\sigma}_{m} \frac{1 - m_{(k)}}{m_{(k)}^{(1+m_{(k)})}} \cdot (\bar{K}^{*}_{I(\varphi)})^{p^{(k)}_{ke}} \quad (2)$$

where $m_{(k)}$ - material strengthening factor, k - number of loading semicycles. For a soft loading the dependance between the low-cycle cracks growth rate (dl^{*}_{ji}/dN) and $(\Delta \bar{K}^{*}_{Ie})_{\varphi}$ is the following (4)

$$dl^{*}_{ji}/dN = C_{\sigma(\varphi)} (\Delta \bar{K}^{*}_{Ie(\varphi)})^{\gamma_{\sigma(\varphi)}} \quad \ldots\ldots\ldots\ldots \quad (3)$$

where l_{ji} - crack length in i direction; N - number of loading cycles; i - direction of coordinate axes X,Y,Z; $C_{\sigma(\varphi)}$, $\gamma_{\sigma(\varphi)}$ - characteristics of material and loading conditions. Fig. 6, 7 and 8 show experimental data on

dependence of low-cycle cracks growth rate in directions i = x and i = Y on values $(\Delta \bar{K}^{*}_{Ie})_{\varphi}$ for two structural steels and elliptic angles $\varphi = 0$ and $\varphi = \pi/2$. Points on these figures correspond to experimental values for cracks with different β at different maximum rated cycle loadings, and the full line - calculated dependance (3). The shown results suggest that parameters $C_{\sigma}(\varphi)$ and $\gamma_{\sigma}(\varphi)$ are constant by crack fronts, thus confirming the proposition (4) that for a wide class of structural steels $\gamma_{\sigma} = 2$. Comparison of fractographic parameters for the studied crack surfaces (Fig. 9) with calculated kinetic-strain characteristics confirmed that the chosen calculation model is correct. The microfocal pattern of fractographic pictures can be explained on the basis of low-cycle crack microtunneling at the stage of its growth according to Model I.

As a result of calculations and experiments, the methodology to study kinetics of surface, semi-elliptic, inclined, low-cycle cracks is developed and tested. Also was proposed and tested the calculation model for surface cracks developed from initial multi-directional surface semi-elliptic crack type notches in the zone of cycle elasto-plastic rated loadings. On the basis of (4), was calculated a dependence to determine strain and stress intensity factors on the front of cracks. Parameters of kinetic dependence C_{σ} and γ_{σ} were found, and their independence on angle β and angle φ was shown. Also, the proposition regarding the universal meaning of $\gamma_{\sigma} = 2$ constant for structural steels was confirmed. Thus, knowing the stress-strain conditions along the front of cracks, it is possible to predict their development in the process of operating the equipment, determine their initial acceptable dimensions, evaluate the equipment service life.

SYMBOLS USED

a and a_1	= greater semi-axes of ellipses (mm)
a^*	= calculation semi-axes for developed crack surfaces (mm)
b and b_1	= smaller semi-axes of ellises (mm)
b^*	= calculation semi-axes for developed crack surfaces (mm)
$C_{\sigma(\varphi)}$ and $\gamma_{\sigma(\varphi)}$	= characteristics of materials and loading conditions
d	= inside diameter of a cylinder (mm)
D	= outside diameter of a cylinder (mm)
$\bar{e}_m$	= relative nominal strain
$\Delta\bar{e}^*_{jz}$	= range of relative elasto-plastic strain on the crack front
$e_{0.2}$	= yield strain
φ	= elliptic angle (rad)
$f(r^*/l^*_{jx})$	= correction function
i	= direction of coordinate axes X,Y,Z
j	= angle β parameter
$\bar{K}^*_{I(\varphi)}$	= relative stress intensity factor in the area of rated elastic strains
$(\bar{K}^*_{Ie})_\varphi$	= relative intensity factor of strain
k	= number of loading semicycles
l_{ji}	= crack length in i direction (mm)
l_p	= external surface perimeter of the sample (mm)
$m_{(k)}$	= material strengthening factor
(dl^*_{ji}/dN)	= low-cycle cracks growth rate (mm/cycle)

N	= number of loading cycles
$P_{Ke}^{(k)}$ and $P_{re}^{(k)}$	= parameters of fracture strain criteria (4)
r^*	= coordinata of the point under study in the minimum section (mm)
t	= cylinder wall thickness (mm)
X, Y, Z	= direction of coordinate axes
β	= angles between the planes of initial semi-elliptic notches and sample cross-sections (rad)
β^*	= calculation angle for developed crack surfaces (rad)
σ_m	= maximum rated cycle stress (Pa)
$\sigma_{0.2}$	= stress of the material yield strength (Pa)

REFERENCES

(1) Sih G.C. Handbook of stress intensity factors. For reseachers and engineers. A catalog of stress intensity factor solution with applications to mixed mode problems. Bethlehem, Lehigh univ., 1973. - 943 p.

(2) Scott P.M., Thorp T.W. A critical review of crack tip stress intensity factors for semi-elliptic cracks. Fatigue of Engineering Materials and Structures. 1981, v. 4, 4, p. 291--309.

(3) Hodulak L., Kordish H., Kuzelman S. and Sommer E. Growth of part - through cracks. ASTM STP 677, 1979, p. 399-410.

(4) Махутов Н.А. Деформационные критерии разрушения и расчет элементов конструкций на прочность. М., Машиностроение, 1981, - 270 с.
Makhutov N.A. Fracture strain criteria and calculation of structurals on strength. M., Machine building. 1981, - 270 p.

(5) Махутов Н.А., Макаренко И.В. Методика исследования кинетики полуэллиптических поверхностных наклонных трещин при малоцикловом нагружении. Заводская лаборатория, том 50, № 2, 1984, с. 63–66.

Makhutov N.A., Makarenko I.V. Methodology to study kinetics of surface semi-elliptic inclined small-cycle cracks. Plant laboratory. 1984, v. 50, 2, p. 63–66.

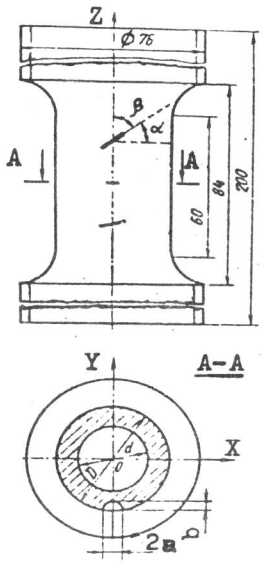

Figure 1 Sketch of a sample with initial notches

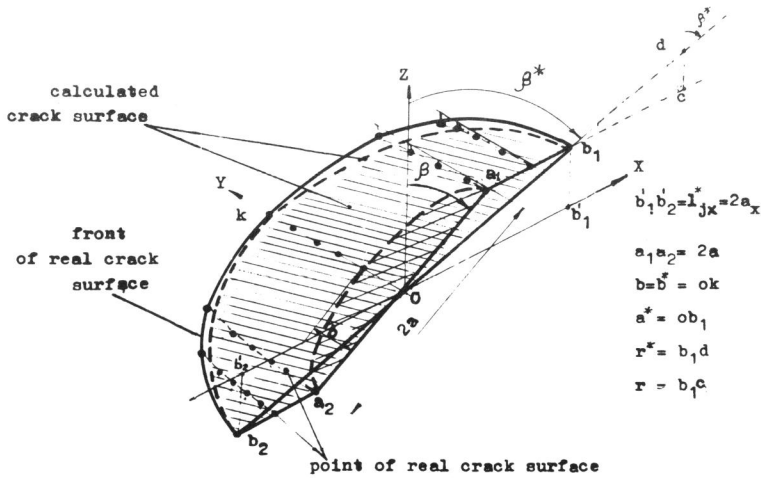

Figure 2 Isometric chart of a surface of crack grown from the initial semi-elliptic notch

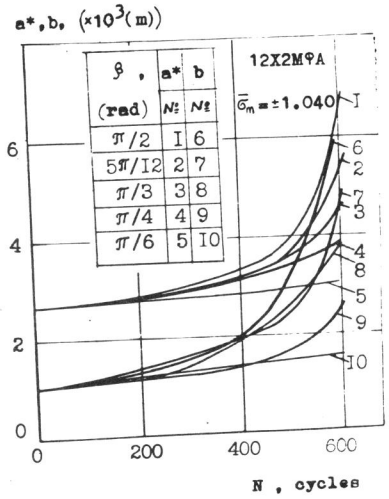

Figure 3 Dependence b and a* on the number of loading cycles N

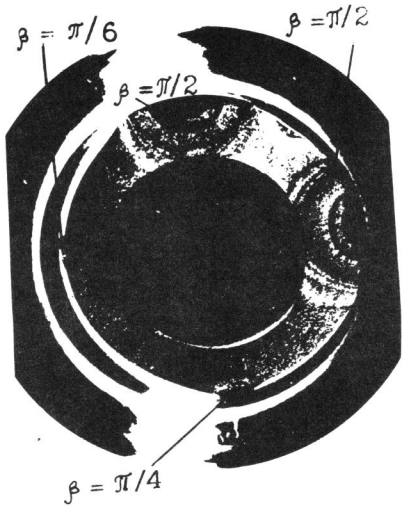

Figure 4 Photo of crack surfaces after complete fracture of the sample

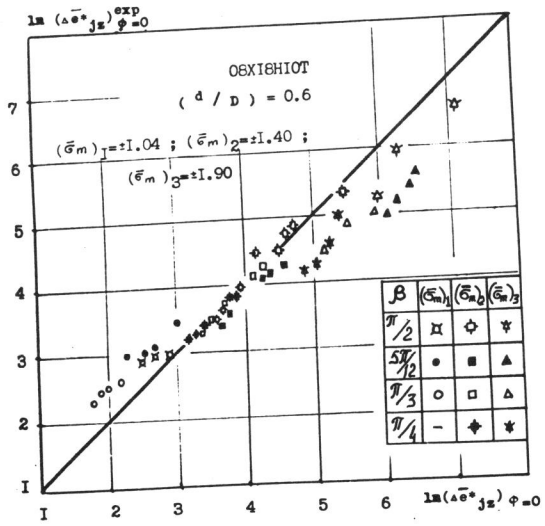

Firure 5 Comparison of calculated and experimental values for ranges of elasto-plastic strains in crack tops

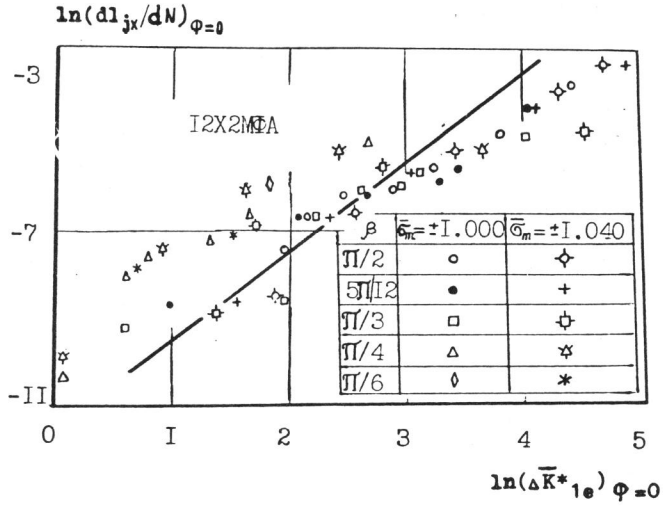

Figure 6 Kinetic dependence of crack growth in i = X direction

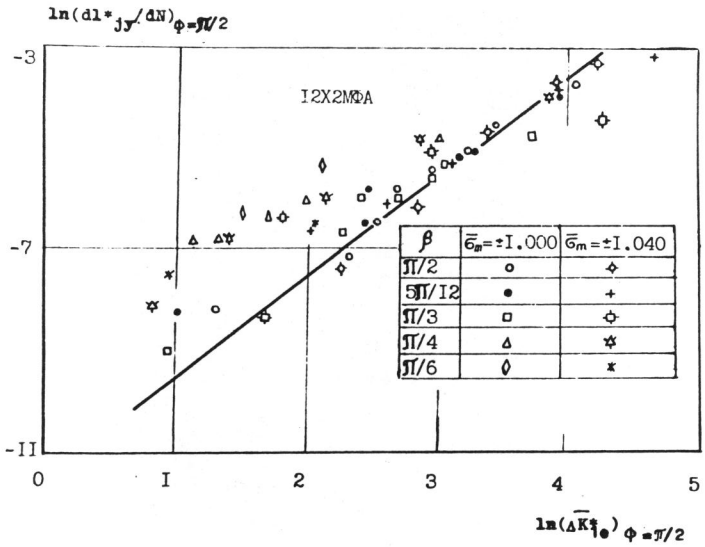

Figure 7 Kinetic dependence of crack growth in i = Y direction

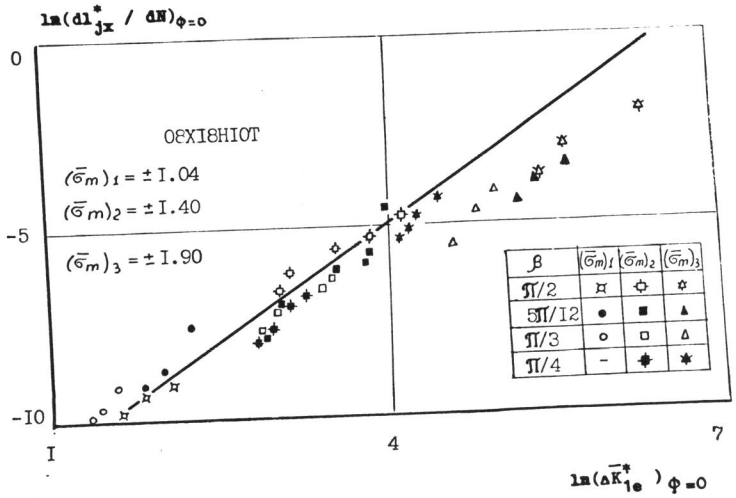

Figure 8 Kinetic dependence of crack growth in i = X direction

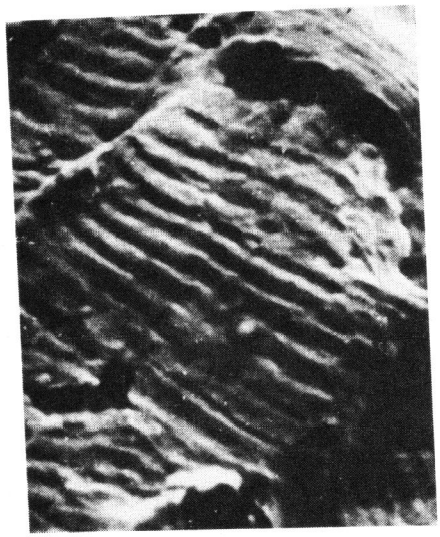

Figure 9 Surface of developed crack with β = π/2 (08X18H10T steel (x5000))